Statistical analysis and optimization for experimental model of output temperature a helical heat exchanger emerging in a cylindrical tank using the response surface method

N. Toujani (toujeninoureddine@gmail.com)
Tunis El Manar University
B. Saleh
Taif University
Nahla BOUAZIZ
Tunis El Manar University

Research Article

Keywords: Helical exchanger, Mathematical modeling, Experimental design, Effects parametric

Posted Date: September 2nd, 2022

DOI: https://doi.org/10.21203/rs.3.rs-1975821/v1

Statistical analysis and optimization for experimental model of output temperature a helical heat exchanger emerging in a cylindrical tank using the response surface method

N. Toujani[1*], B. Saleh[2], Nahla BOUAZIZ[1]

[1] Tunis El Manar University, National School of Engineers (ENIT) of Tunis, Energy Research and Environment Unit, , BP 37, Le Belvédère1002 Tunis, Tunisia

[2] Mechanical Engineering Department, College of Engineering, Taif University, P.O. Box 11099, Taif 21944, Saudi Arabia

[*] Corresponding author Email: toujeninoureddine@gmail.com

Abstract

In this study, the performance of the helical coil heat exchanger is experimentally tested. The results are statistically analyzed using the response surface methodology (RSM) to optimize the heat exchanger response under various parameters. The helical coil outlet temperature is measured as the heat exchanger response. The considered parameters, affecting the performance, are the inlet temperature and pressure to the helical coil in addition to the water bath temperature surrounding the coil. Also, the mutual interactions between these parameters and their influences on the response of the helical coil are evaluated. This study is carried out in two parts, the first part is devoted to perform the experimental tests, and the second part deals statistically with the modelling and optimization of these results. Design of experiments (DOE) is provided according to the full factorial design method. Three parameters with three levels lead to performing 27 experimental runs. Finally, the results are modelled by the RSM method, and the adequacy of the model is verified by ANOVA analysis. The analysis of each parameter effect was performed to identify and rank various critical parameters relative to their order of importance. A complete RSM statistical model with a full factorial design is established. The results show that the statistical model equation has an accuracy of more than 98% to predict the output response of the heat exchanger. The inlet temperature has a dominant effect on the response by 30%. The mutual combination between the investigated parameters shows that the most important correlation is between the inlet temperature and pressure. The developed model enables the optimization of the outlet temperature response without referring to the physical and thermal properties of the used fluid.

Keywords: Helical exchanger; Mathematical modeling; Experimental design; Effects parametric.

Abbreviations

CCF: Centered Composite Face
CED :Complete experimental design
DOE: Design of Experiments
DW: Durbin-Watson
GSHP: Ground source heat pump
Hmp: Total head of the pump
IEA: International Energy Agency
MAE: Mean absolute error
PCM: Phase Change Materials
RSM: Response Surface Methodology
TES: Thermal energy storage

Symbols

D: Diameter of turn of the exchanger
d: Diameter of exchanger tube
E: Tube thickness of the helical exchanger
Ns: Number of turns of the helical exchanger
p_1: Pressure
Pu: Electric power of the pump
T_a: Ambient temperature
T_h: Temperature of the water tank
T_i: Helical tube inlet temperature
T_o: Helical tube outlet temperature
V: Tank volume

1. Introduction

According to the International Energy Agency (IEA), solar power becomes one of the fastest-growing sources of energy in the future. The solar energy growth rate could reach more than 12% (IEA, 2010) [1]. Today, several countries decided to put political strategies in the utilization of renewable resources. Accordingly, several studies were conducted all over the world, America [2], Africa [3, 4], Asia [5, 6], whose goals are to find the energy potential and to select the political strategies to enhance the benefit from the solar energy potential. In Europe 2014 [7], a target was set to increasing the energy efficiency by 20 % and 30% by 2020 and 2030 respectively. In fact, researches are devoted to technologies that can be utilized to alleviate global warming and decrease emissions of CO_2 [8]. On the other hand, there is a shortage in energy facing the world and representing obstacles in all fields [9, 10]. Consequently, the world faces two energy challenges; increasing production to meet the requirements and reducing emissions from industrial plants. So, the usage of renewable energy becomes a political duty and not just a strategic choice to solve energy problems. Amongst the renewable resources, solar energy comes in the lead; Sunil Kumar and Sharma [11] published a comprehensive review on the solar energy analyses. They showed several solar energy systems utilized in refrigeration [12], air conditioning [13, 14], water heating [15], cooking [16], and drying [17, 18]. These systems are activated by solar photovoltaic panels [19] or solar thermal energy collectors [20-22].

Heat exchange represents the core of constructing a system to use solar energy and other variety of renewable energy sources such as geothermal energy, which initiates the necessities to design an efficient heat exchanger. The vertical helical exchanger is used mainly in the solar field to heat the water in a storage tank and in geothermal energy to recover the underground thermal energy. The helical tube type occupies less area, supports a very long pipe length with maximum performance in cold regions [23-27]. While the U-tube type may be selected due to its ease of installation regardless

of the size limitations and the high cost compared to the helical type [24]. Based on the stated advantages, the helical tube type is the subject of this study.

Several researches were carried out on the vertical helical exchanger performance experimentally and mathematically. In the geothermal application, Carotenuto et al. and others [25-27] studied numerically the heat transfer through the U-tube, Double U-tubes, Triple U-tubes, and helical coil using a mixed 1D-3D approach. Zhou et al. [28] and Li et al. [29] investigated the effect of Reynolds number on the performance of the U tube exchanger. The results showed that the recommended Reynolds number found for a U tube exchanger operated in geothermal is in the range of 12000 to 21000.

The numerical models are developed to simulate the geothermal U tube exchanger. Bauer et al. [30] developed a 2D finite-difference model to study the thermal resistance and capacity of borehole heat exchangers. While Al Khoury et al. [31, 32] introduced two finite element models to simulate the steady-state and transient performance of geothermal heating systems. He et al. [33] presented a 3D numerical model based on finite volume for circulating fluid in borehole heat exchangers.

For the interest of simulation of phenomena of the vertical helical heat exchanger, exactly in the geothermal operation, Comsol [34] developed a finite element numerical model for the buried geothermal pipes. The model simulates the fluid circulation through the vertical-type helical heat exchangers. Florides and Kalogirou [35] reviewed the evolution and description of different types of ground heat exchangers and the models utilized in the literature to simulate the heat transfer process. Yang et al. [36] gave a review of the vertical Vertical-borehole ground-coupled heat pumps and the related simulation models for the vertical ground heat exchangers. A finite-difference model including phase change material was established to investigate the transient performance of solar-assisted energy storage tanks [37].

Shirvan et al. [38-40] studied the effect of input parameters on the performance of the solar heat exchanger. They investigated numerically, with help of RMS, the effect of nanoparticle concentration effects on natural convection coefficient and entropy generation. Also, Shirvan et al. [41] performed a sensitivity analysis of the heat transfer effectiveness using Al_2O_3 nanoparticles and the results are analyzed using the Response Surface Methodology (RSM) method. The RSM is a decision technique that makes it possible to evaluate and validate such as design or the choice of operating parameters. The selection principles mainly occur in the choice of optimum objective functions based on evaluation functions at some different points in the design (Geometry and operating conditions). The use of structured optimization based on experimental design became essential in-process and structural engineering. Many thanks are devoted to its faster scripting and better programming routines provided by scalable capabilities. Also, the response methodology

surfaces are perfectly modeled by objective (the most common) polynomial functions which are adapted to assess the objective values in the design considered in space with finite geometries. This avoids performing unlimited tests to determine the optimal solution in all the surfaces representing the variation of physical factors controlling the structures and processes.

Based on the literature, the multi-response optimization of helical coil type exchanger using RSM based on experimental test has not yet been considered. In this study, the multi-response optimization of heat transfer characteristics including the outlet temperature is performed by the RSM using the desirability function approach. Results based on experimental tests and statistically analyzed to optimize thermal performance using the RSM. In the following sections, the description of the experimental system and experience plan methodology, and multi-response optimization due to the exchanger are explained in detail.

2. Method and study goals

2.1. problematic

The helical heat exchanger is frequently used in industrial applications to recover or transfer a quantity of heat at high or low temperatures. The process of heat transfer is generally done by convection where the conduction effect is too weak. One of the major applications in the market, the helical heat exchanger is used to transfer solar heat captured by a solar panel to the hot home water. The home sanitary water is circulated in a tank while the solar panel hot water is circulated in a helical exchanger immersed in this tank. **Figure 1** shows an explanatory diagram of the circulation process in a helical heat exchanger which comprises a helical-shaped copper tube immersed in a cylindrical tank.

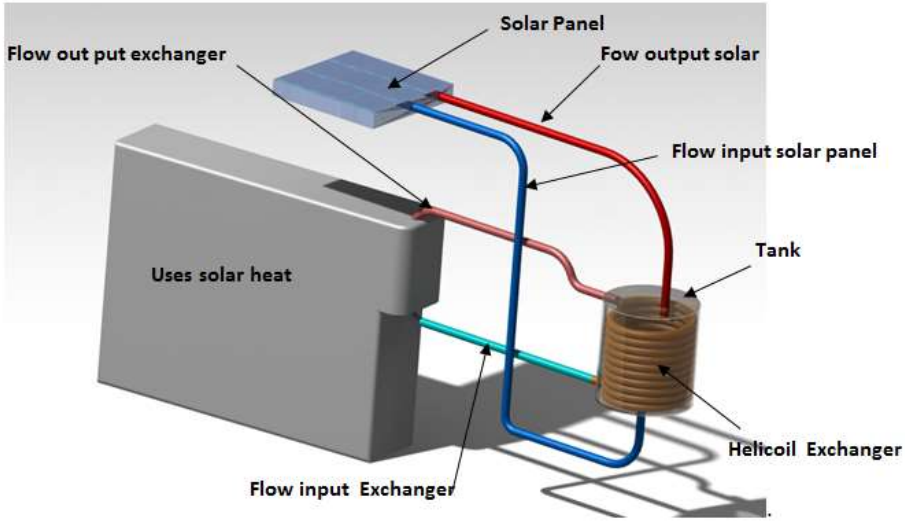

Fig. 1. Descriptive 3D of solar application of the helicoil exchanger.

Today, the industry is looking for the optimization of the operating parameters of this mode of application. The optimization technique requires careful tuning of a number of parameters in order to reach the optimum operating conditions of the exchanger which leads to improve the overall performance. But, before applying the optimization, it is essential to identify the influencing parameters and the desired performances. To facilitate the continuous improvement of the exchanger, it is necessary to implement a practical empirical model based on experimental tests which develop an analytical performance function related to the operating parameters and their degrees of effects.

In the present study, the objective is to establish an experimental test rig to study the out-put temperature of a helical exchanger as a function of input parameters. The considered input parameters are inlet working pressure (the flow rate motivation), reservoir temperature, and inlet temperature at the coil tube exchanger. Consequently, the RSM is used to model and optimize the output temperature response surface according to the impact and interaction of these input parameters on the output temperature performance.

2.2 Goals of the study

The objectives of the present work are:

- Realization of an experimental Test.
- Statistical analysis of operative parameters and responses.
- Modeling and analysis of the heat transfer characteristics of a helical exchanger, notably the output temperature, using a statistical model RSM with reference to three input design parameters namely the inlet temperature and the reservoir temperature, and the inlet working pressure.
- Identification and classification of different critical parameters for heat transfer characteristics of the exchanger with respect to their order of importance utilizing sensitivity analysis.
- Prediction of optimal temperature output and determination of optimal levels of input parameters using the multi-response optimization technique.
- Response surface analysis and model validation.

2.3 Methodology

In order to achieve our desired objectives, a plan of synchronized and ordered processes for the present study is developed. **Figure 2** displays the flowchart that describes the study phases with their method and sequence.

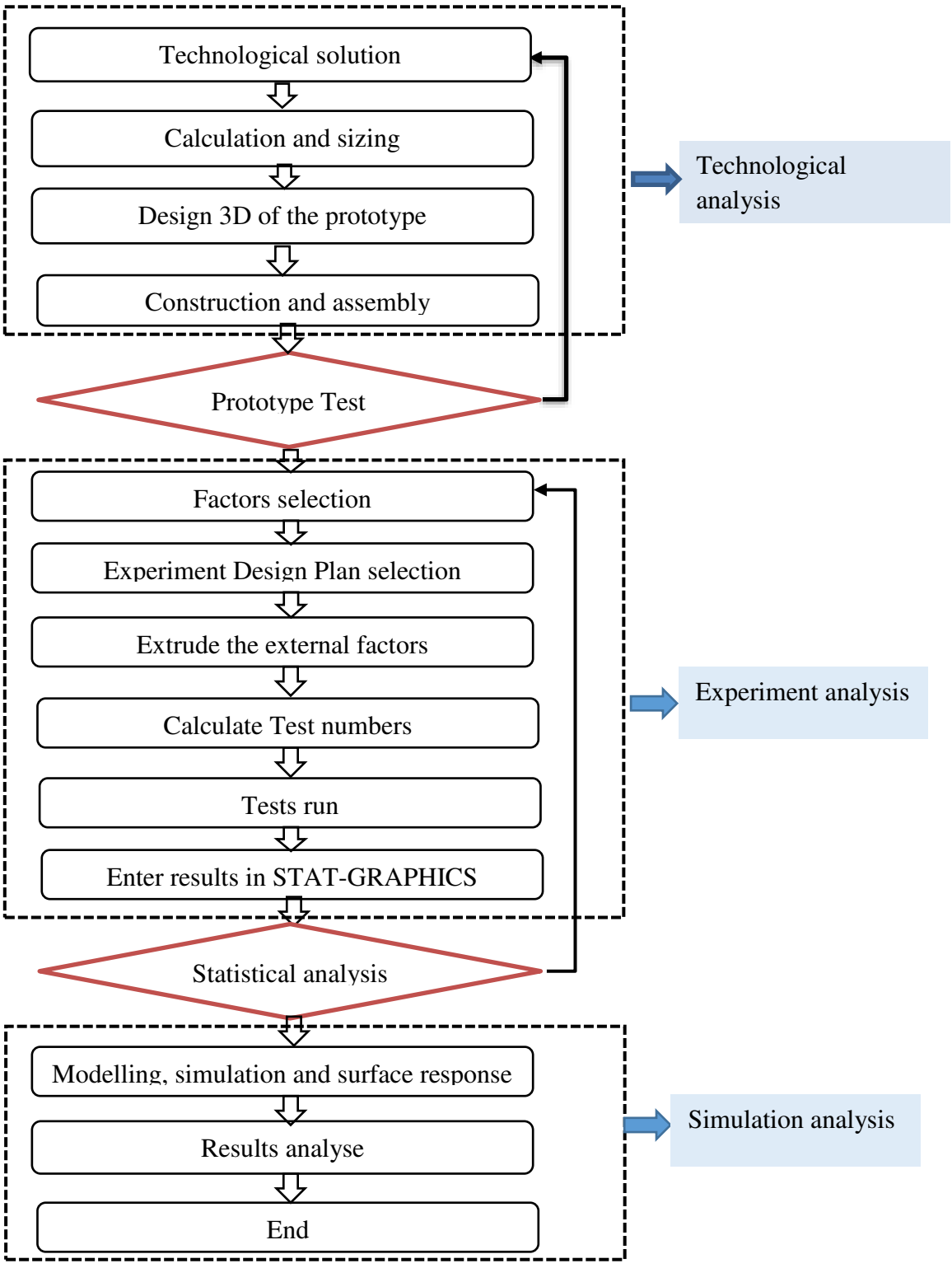

Fig. 2. Process and methodology.

In this study, special attention is given to optimizing the output temperature. The optimization of the helical coil is done with the help of experimental data. **Figure 3** illustrates the detailed information on the geometrical shape of the exchanger coil. All dimensions of the exchanger section are listed in **Table 1**.

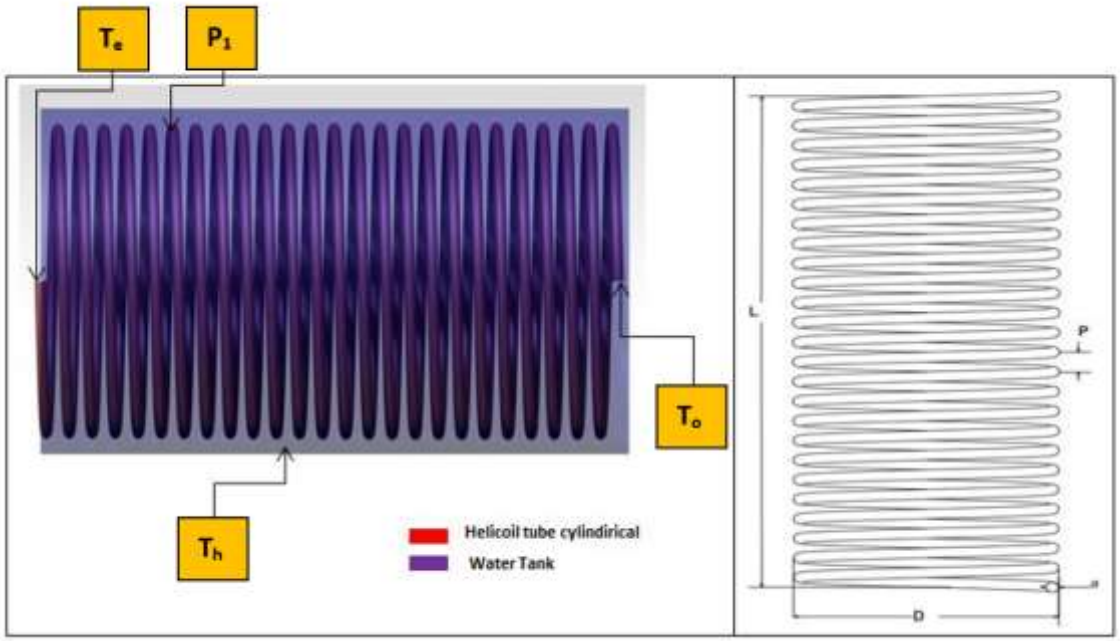

Fig. 3. Shape and geometrical dimensions of the exchanger.

Table 1. Experimental parameters and geometric characteristics of the exchanger.

Experimental parameter of the exchanger					
General parametric			Specific parametric		
Parameter	Symbol	quality	parameter	Symbol	Quality
Turns number	Ns	10	Hot temp. of the water tank	T_h	40-60 °C
Pitch	P	25 mm	Tank volume	V	10 l
Material		Copper	Diameter of turns	D	200 mm
Thickness	E	1 mm	Inlet water temperature	T_i	15-25 °C
Electric power of the pump	Pu	0.5 kw			
Maximum pump head	H_{mp}	40 m			
Ambient temperature	T_a	13 °C			

3. Test rig description

Figure 4 displays a photograph of the implemented test rig equipped with the basic components. The flow circuit diagram of the test rig and the installed transducers are shown in **Fig. 5**. The working principle is described as follows: The main pump draws the liquid water from the main tank at atmospheric pressure and discharges it at the exit pressure. Then, the water passes through an insulated copper pipe to a manually adjustable expansion valve to set the desired pressure. Once the pressure is set and its value is displayed by the manometer, the water passes into the helical

coil immersed in a water tank which representing together the helical heat exchanger. The helical heat exchanger has an electrical resistance used to heat the water in the tank to the required T_h. Varying and controlling the hot temperature to the required value are attained by the potentiometer mounted in the test rig board and the probe immersed in the hot water bath. After going through the helical exchanger, the water outlet temperature from the coil is raised and then required to be cooled before returning to the main tank. A cross-current air exchanger is integrated to cool it down. This exchanger consists of a bank of tubes mounted in a rectangular shape where the water exit from the exchanger will be circulated in these tubes to cool down to room temperature. The required cooling air is delivered by a fan equipped with a speed controller to properly cool the variable outlet temperature from the exchanger to room temperature. For any circumstances, a supplementary exchanger tank is used to guarantee that the exit temperature from the air exchanger reaches the ambient condition before discharging into the main tank. The flow and electric components allow the appropriate choice of the required inlet parameters to have steady-state correct system operation. Finally, the water goes to the main tank at ambient temperature to redistribute it.

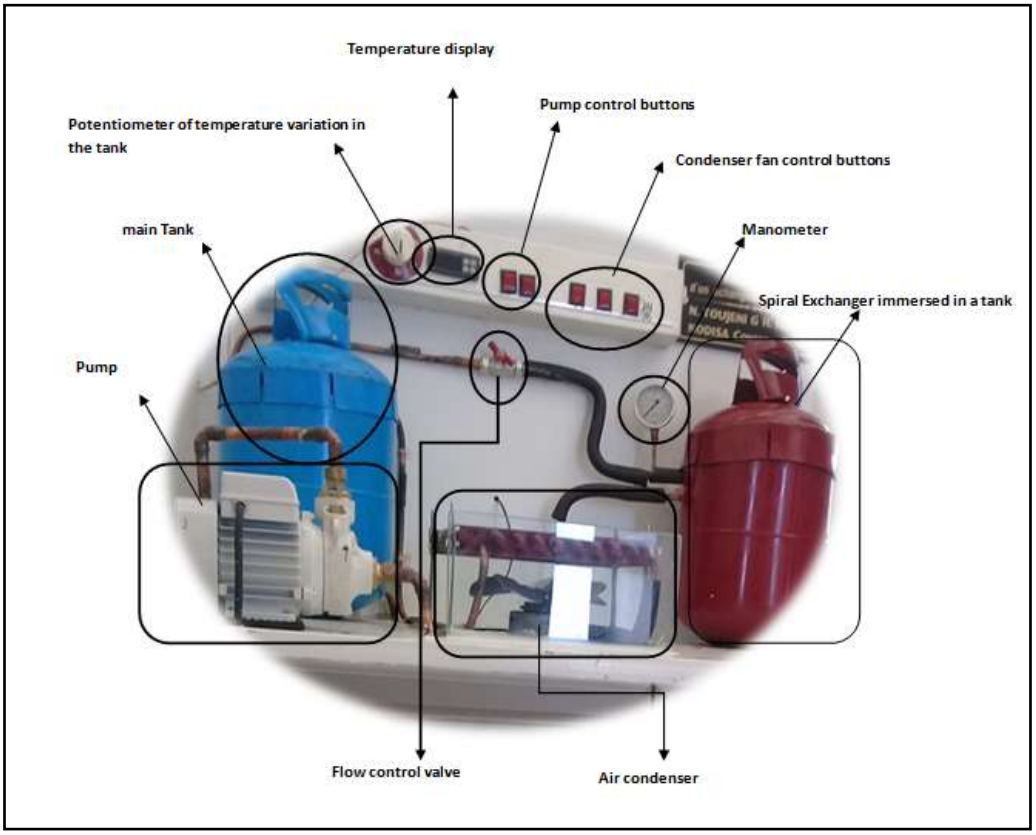

Fig. 4. Experimental test rig.

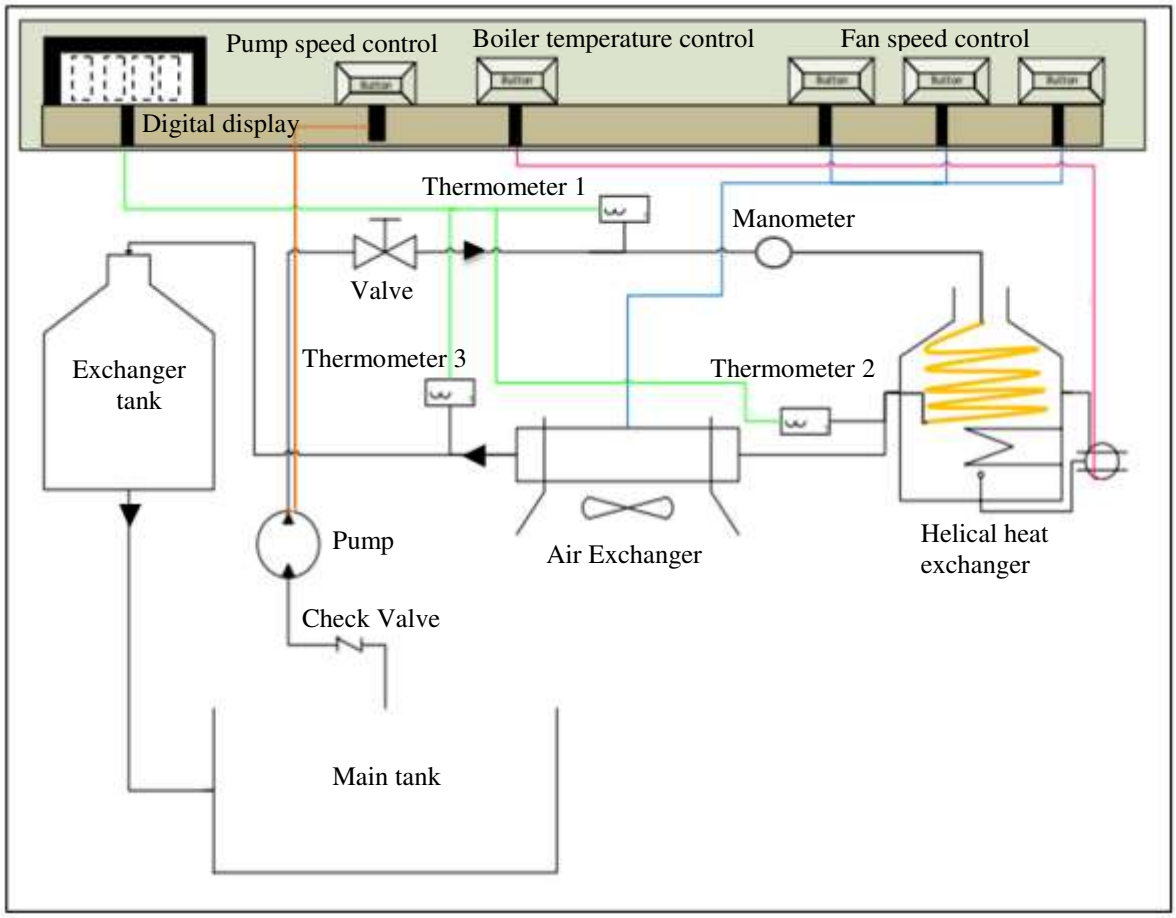

Fig. 5. Hydraulic circuit diagram of the experimental test rig.

To ensure a proper operation, the test rig is equipped with: (i) An anti-return valve mounted just above the tank to ensure water flow direction, (ii) One meter to measure pressure, and (iii) Four measurement points linked to a thermocouple are used to measure and control the temperature.

4. The response surface model and experimental test execution

4.1. Approach and concept of RSM

The conventional methods for optimization, such as computational fluid dynamics CFD, address one factor at a time, consume a lot of time, and cannot evaluate the response due to the interaction effect of two or more variables. While the RSM can predict the relationship of the effects and interactions of different input parameters on a set of response variables with the smallest number of experiments and in less running cost. The RSM is a frequent optimization method used in the industry for modeling and analyzing engineering problems. This technique is based essentially on mathematical and statistical concepts that can be applied to the data obtained from the process.

Several input variables (independent variables) potentially affect the desired output performance or quality (dependent variable) of the product or process. This output performance or

quality is known as the response. Normally, the relationship that describes both the individual and the interaction effects of the independent variables on the response is unknown. The RSM can be used to establish the approximate mathematical function that describes properly the relationship between the independent variables and the process response. **Figure 6** displays the inputs and the outputs of the RSM method in a simple flowchart.

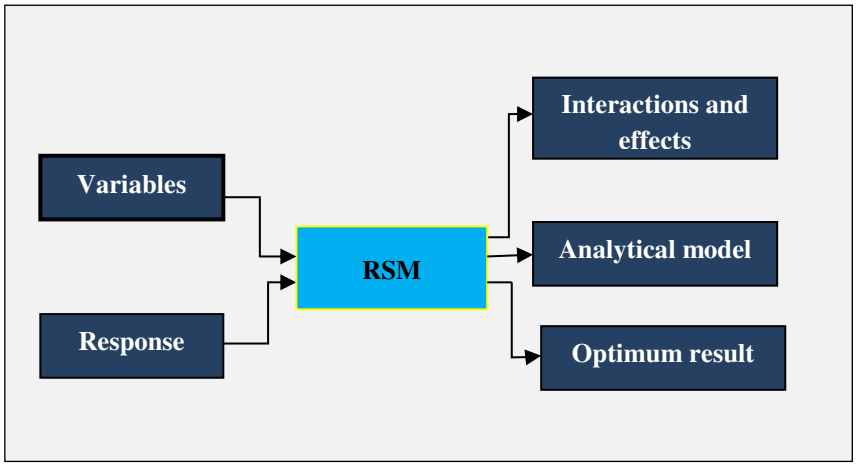

Fig. 6. Inputs - Outputs of the RSM method.

To analyze, predict, and optimize the process, the commonly used method by researchers is the mathematical modeling based on RSM with selecting one of the designs of the experiment (DOE) plans aiming to evaluate the effects and interaction of variables on the process output response [42-45]. The RSM is a global optimization algorithm that includes a set of techniques, namely, DOE, regression analysis, and validity of data by analysis of variance (ANOVA). The DOE is a tool that can be used to specify the minimum number of experiments to scan the effects of the independent variables and their interactions on the process output response. The Regression analysis is a statistical method to generate the relationship between dependent and independent variables and examine the impact of variables on the output response. The Analysis of Variance (ANOVA) is a statistical method that checked the adequacy of the fitted model using F-test which indicates if your linear regression model provides a better fit to the data than a null hypothesis that contains no independent variables. A common method for testing the significance of a response surface model is the adjusted coefficient of determination (R^2adj). It is suggested that, when R^2adj is more than 0.9, the output values are accurately predicted by the response surface model.

4.2. Experiment design and factor levels

Mathematical rules and a rigorous approach of the experiment design are set to obtain the maximum of information with the minimum of experiment runs. There are many types adapted to fit all encountered experimental cases such as general full factorial, fractional factorial, Central Composite Designs, Box-Behnken, Taguchi, etc. The use of the RSM with the application of the general full factorial design provides a large amount of information on modeling and optimization of the process. The fundamental principles of this art will be indicated later. The design of experiments is based on two essential domains, one is the experimental space identified by the factor level values and the other is the mathematical modeling of these values.

Full factorial designs are the first test planning tools that were developed in the early 20th century. They are the only methods able to consider all the input factors interactions, and consequently, avoid the misleading of any combination that may affect the output response. Also, they are the most technically simple; well suited to the introduction of methodological elements; and they are often used due to their precision. **Table 2** shows the values of three encoding levels (low (-1), center (0), and high (1)) for each independent factor which delivered to STAT-GRAPHICS software. For more precision and more confidence in results, the general full factorial is adapted for the present work.

Table 2. Coding of study parameters.

Parametric	Notation	Code	levels		
			(-1)	(0)	(1)
pressure (bar)	p_1	p_1	0.5	1	1.5
Inlet temperature(°C)	T_i	T_i	15	20	25
Temperature of the water tank (°C)	T_h	T_h	40	50	60

4.3 Experimental tests and execution

The working conditions during the execution of the tests are as follows: Ambient temperature is 15 °C; humidity is 65 %, the attitude is 627 m, working fluid is water, and the time between two tests is 50 min. For full factorial, the number of tests required for n factors with k levels is k^n trails. In the present study, 3 factors with a 3-level full factorial design require 27 trials. Concerning the recorded measurements for each experiment, each trail has been repeated five times at the same working condition, afterward, the average T_o is recorded to ensure the accuracy and confidence of this output response of the system. **Table 3** shows the complete full factorial trails with their experimental output temperatures.

Table 3. Table of complete design of experiment with response temperatures.

Trial	p_1	T_h	T_i	T_o
1	-1	-1	-1	21.4
2	0	-1	-1	20.2
3	1	-1	-1	19.9
4	-1	0	-1	26.5
5	0	0	-1	24.1
6	1	0	-1	22.6
7	-1	1	-1	29.4
8	0	1	-1	26.9
9	1	1	-1	25.3
10	-1	-1	0	26.6
11	0	-1	0	25.2
12	1	-1	0	24.9
13	-1	0	0	29.4
14	0	0	0	27.5
15	1	0	0	25.6
16	-1	1	0	33.2
17	0	1	0	30
18	1	1	0	28.5
19	-1	-1	1	30.1
20	0	-1	1	29.4
21	1	-1	1	28.8
22	-1	0	1	34.8
23	0	0	1	32
24	1	0	1	30.6
25	-1	1	1	37.2
26	0	1	1	32.3
27	1	1	1	30.2

5. Result and discussion

Experimental results for the output temperature were assessed using Statgraphics Centurion statistical analysis software following the full factorial scheme in the RSM to estimate the impact of the input factors on the exit temperature. The following subsections discuss the effects of the factors and their combination on the evolution of the exit temperature from the heat exchanger coil immersed in a cylindrical tank of water. Empirical models of the optimization and the response surfaces will be presented and interpreted.

Each regression method has some assumptions that must be verified to ensure the applicability of them to be supposed in the case study. The assumptions of the ordinary least squares regression model are:

- The model should be linear.
- The data should be randomly sampled.
- Explanatory variables should not be collinear.
- The explanatory variables must present a negligible measurement error.
- The expected sum of residuals is zero.
- The variance of the residuals is homogeneous.
- Residuals are distributed normally.
- Adjacent residuals must not show auto-correlation.

5. 1. The multiple regression method

The regression analysis investigates the relationship between the quantitative output response and one or more independent (explanatory) variables and named simple or multiple regression respectively. First-order, quadratic and even cubic interpolations can be adopted to model the physical phenomenon of a given application. The model order is identified to reflect how accurately the model equation fits the data and predicts the output response. The adequacy of the fitted model is checked by ANOVA using Fisher F-test. There are two hypotheses namely the null hypothesis where all the model coefficients equal zero and the alternative hypotheses where at least one coefficient is not zero. Comparing the value of $F_{\text{calculated}}$ with F_{critical} obtained from the tables according to the significance level value(α). If $F_{\text{calculated}} > F_{\text{critical}}$, the null hypothesis is rejected. The existence of β coefficient of the alternative hypnosis is considered base on the Probability plot $(P - \text{value})$ which shows that the variable has a correlation with the dependent variable or can be excluded. Consequently, modeling of the response surfaces by general quadratic polynomial approximation will be written as:

$$\hat{y} = \beta_0 + \sum_{i=1}^{n} \beta_i x_i + \sum_{i<j}^{n} \beta_{ij} x_i x_j + \sum_{i=1}^{n} \beta_{ii} x_i^2 \quad (1)$$

where $\hat{y}$ is the response function where the difference between the measured data (y) and the predicted response $(\hat{y})$ is the regression equation error(ε), x_i , x_j are the adjustable independent factors of the process to be modeled, n is the number of factors, the polynomial coefficients are β_0, β_i, β_{ii}, and β_{ij} epresenting the y-intercept, the coefficients of linear terms, the coefficients of quadratic terms, and the coefficients of interaction terms, respectively.

5. 2. The Validity of the model and confirmation analysis

The adequacy of the regression equation represents a crucial role in optimization analysis. All models include some margin of error, but the well posed statistics can identify the degree of suitability of the model and the adjustments that need to be made. The exploratory analysis uses a set of visual and statistical techniques to analyze the data model. During exploratory analysis, the ordinary least squares regression is tested and the effectiveness of the different explanatory variables are compared. The following diagrams and statistics can be used for exploratory analysis: Fisher F-test, Regression equation and forecast of new observations, Coefficient of determination, R^2 and R^2 adjusted, Pareto chart, Standard residual error, and Normal probability diagram

The final ANOVA factorial experiment is shown in **Table 5**. Actually selected regression method, there are 9 source terms in the model equation representing $x_i,\ x_i x_j,$ and x_i^2. The variability of T_s for only significant estimate effects and interactions are presented in table 5. The excluding principle of insignificant source terms will be shown later using Pareto chart. The F-ratio is the ratio of the mean square of regression residual ($MS_{regression}$) over mean square of total error ($MS_{total\ error}$). The F statistic is a universal statistic returned by an F test, which shows the forecasting capacity of the regression model by finding if all the regression coefficients of the model are significantly different from zero. The F test analyzes the combined effect of the explanatory variables, rather than testing them individually. The F statistic is associated with a P-value, which shows the probability that the relationships in the data are the result of chance. Since P-values are based on probabilities, the values are given on a scale from 0.0 to 1.0. A low P-value, typically 0.05 or less, is required to determine that the model relationships are not accidental and to rule out the hypothesis nothing. In another word, the probability that the model relationships are the result of chance is 5% or the confidence that the model relationships are real is 95%.

From the critical F-distribution table, the $F_{\text{critical}} = 4.3512$ at source degree of freedom DF = 1 and total error degree of freedom DF = 20. As shown in **Table 4**, the condition $F_{\text{calculated}} > F_{\text{critical}}$ is satisfied for the six significant source terms in the regression equation. Also, the significance of each source is tested by comparing the calculated probability P-value with the significance level of 0.05 at the 95.0% confidence level. In this case, six terms have P-values less than 0.05, which confirms the rejection of null hypnosis and shows that they are significantly altered from zero.

Table 4. Estimate effects and interactions.

Source	Sum of squares	DF	Mean Square	F-ratio	P-value
A: p_1	57.6022	1	57.6022	151.77	0.0000

B: T_h	120.125	1	120.125	316.51	0.0000
C: T_i	265.267	1	256.267	698.94	0.0000
AA	1.77852	1	1.77852	4.69	0.0427
BB	10.6408	1	10.6408	28.04	0.0000
BC	6.3075	1	6.3075	16.62	0.0006
Total error	7.59065	20	0.379528		
Total error (corr.)	469.312	26			
R squared = 98.3826%					
R-squared (adjusted of d.f.) = 97.8974 %					

The coefficient of determination, symbolized by R^2, measures how the regression equation predicted the variability in the actual data points. The R^2 value is a number between 0 and 1. A value R^2 equal to 1 indicates a perfect model, which is highly improbable in real situations, demonstrated the complexity of the interactions between different factors and the unknown variables. While the value of 0 indicates that none of the variability in the data can be explained by the predicted model. As the R^2 value approaches 1, this indicated that the predicted model has greater accuracy and describes all of the variability in the data. It should therefore strive to create a regression model with the highest R^2 value as possible, while accepting that this value is not equal to 1.

When performing a regression analysis, the attention is devoted toward create a pure regression model whose value R^2 is acceptable by adding explanatory variables that trigger a better match. The adjusted R^2 reveals the percentage of variation explained by the independent variables that significantly affected the dependent variable. Also, its value is between 0 and 1. The adjusted R^2 value should be used for models that use many explanatory variables or to compare models with different numbers of explanatory variables.

The R-squared statistic indicates that the adjusted model explains 98.3826% of the variation of T_o. This means that more than 98% of the data fit the regression model. The adjusted R-squared statistic, which is more relevant for comparing models with different numbers of autonomous variables, is 97.8974%. This percent shows the degree of good fitness between well the multiple regression equation and the experimental data. The regular error of the assessment shows that the standard deviation of the residues is 0.616058.

The Durbin-Watson test measures the autocorrelation of the residuals in the regression model. The Durbin-Watson test uses a scale of 0 to 4. The interpretation of the scale is divided into three parts. First, the values between 0 and less than 2 indicate a positive auto-correlation, the second the value of 2 indicate the absence of auto-correlation, while the values between 2 and 4 indicate a negative correlation auto-correlation. Therefore, values close to 2 are necessary to satisfy the assumption that there is no autocorrelation of the residuals. In general, values between 1.5 and 2.5

are considered acceptable, while values less than 1.5 or greater than 2.5 indicate that the model does not meet the non-correlation assumption.

The mean absolute error (MAE) of 0.444239 is the mean value of the residues. The Durbin-Watson (DW) statistic tests the residuals to determine if there is a significant auto-correlation based on the order in which they appear in the data file. The calculated DW value is 1.5948344 which is bigger than 1.5. This result concludes that there is probably no serious autocorrelation in the solutions. The following statistical outputs are utilized to find relevance for the confirmation analysis: Statistic F and its associated P-value, Statistics t and their associated P-values, and Confidence Intervals.

In screening assays, all the effects of factors (first and quadratic) and all possible interactions are considered into account as shown in the Pareto result graph of **Fig. 7a**. The results show that the interactions AA, AB, and BC above the Pareto threshold represented by the blue line are significant. Accordingly, we proceed by relaunching the analysis of the variance (ANOVA) by eliminating the interactions BB, AC, and CC which have non-significant effects on the output response. The dedicated result of this new ANOVA analysis via the Statgraphics Software is displayed in **Fig. 7b**. The predicted model, shown in **Fig. 7b**, is readjusted to only contain the effects of the significant independent variables which minimizing the residual and the error of the model response T_o. The Pareto diagrams (raw and optimized) reveal that the inlet temperature has the primordial and major effect on the evolution of the temperature T_o with an approximate rate of 28%. Furthermore, the hot path temperature has an effect of 20% and the actuating pressure has an effective rate of 14%.

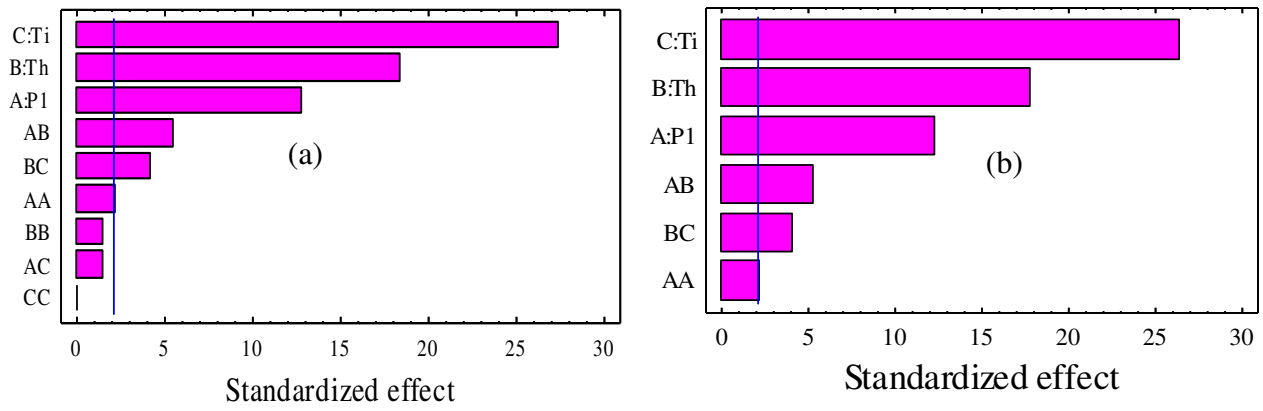

Fig. 7. Pareto chart for T_o, (a) Pareto raw and unoptimized, and (b) optimized Pareto.

This standardized effect of the optimized Pareto variables is confirmed in **Figs. 8** and **9** by plotting the response To against these variables and their significant interactions. **Figure 8** reveals the major effect of inlet temperature T_i on T_o. The range of T_i from -1 to +1 exhibits a large range of variation of T_o from 23 °C to 32 °C compared with the other two factors that have a range of variation

of T_o from 25 °C to 29 °C. Moreover, the range of variation of T_o with the interaction between these factors is shown in **Fig. 9**. The four interaction curves do not have a secant and close to the limit, it is observed that the A-B interference is closer to B-C. This leads to the conclusion that the effects of the variables themself are more significant than their interaction effects and that the A-B interaction is more significant than B-C.

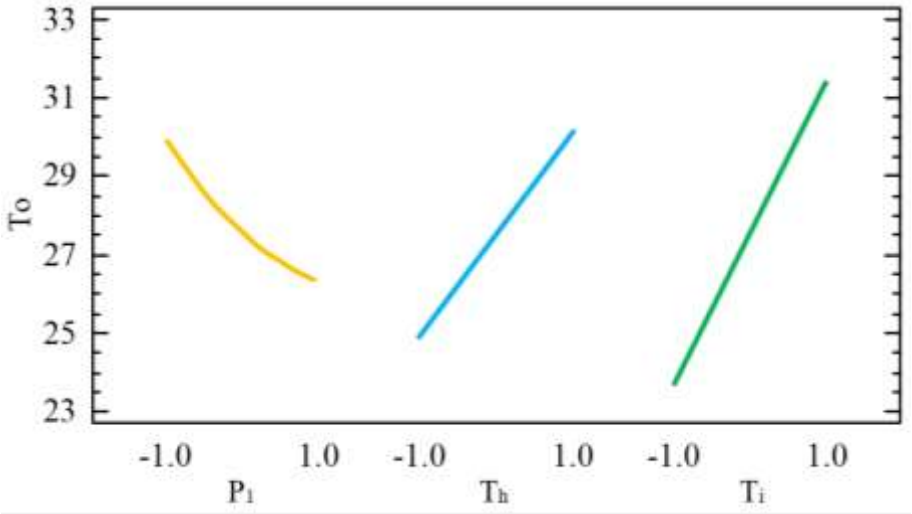

Fig. 8. Effects parametrics.

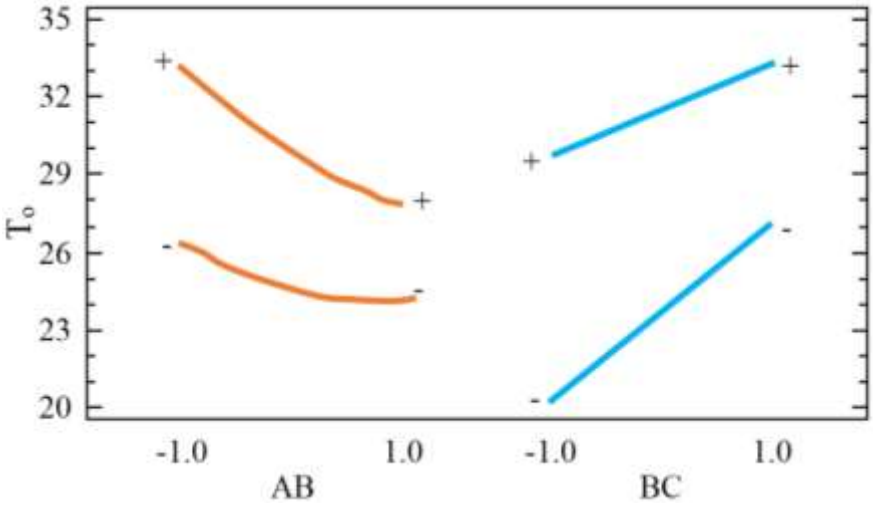

Fig. 9. Interaction plot for T_o.

In a regression analysis, the residuals are correspond to the difference between the experimental and the model predicted values. The points located above the regression curve have a positive residual value while the points located below the regression curve have a negative residual value. Therefore, the accepted regression curve should lie along with the mid-range of these data points, and consequently, the sum of the residuals must be zero with the same variance for all

residuals. This hypothesis can be tested utilizing a point cloud of residuals (y-axis) and estimated values (x-axis). The point cloud generated should be displayed as a horizontal band of points plotted randomly across the entire plot.

Figure 10 illustrates the normal probability plot of the residual. It is perceived that the measured points follow the theoretical line of the model which is almost passing through halfway. Thus, it can be concluded that the residual values verify the normal distribution assumption and the suitability of fitting both ANOVA and regression model. Therefore, the model can be adapted and applied along with the range of studies with a good resolution.

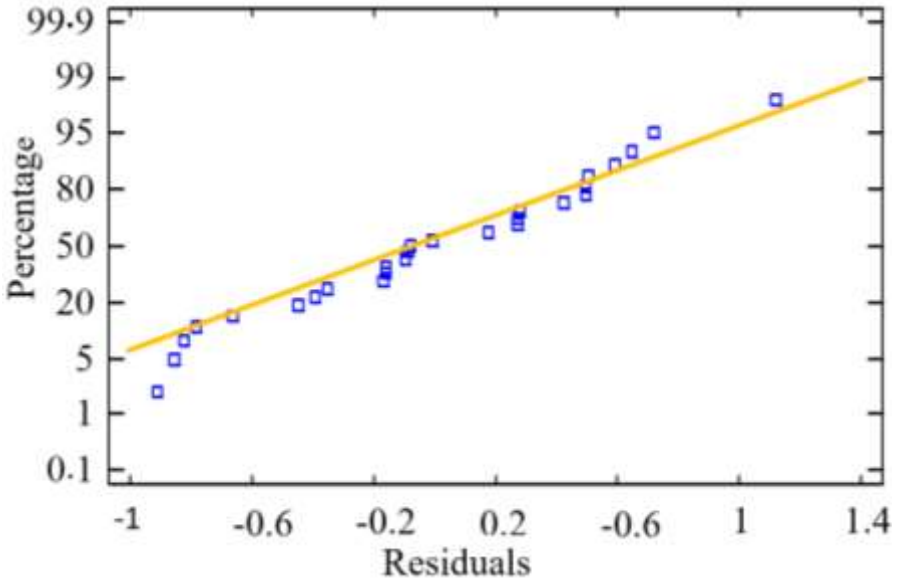

Fig. 10. Normal probability plot for residuals.

The considered three factors to lead the experiments of the exit temperature of the helical exchanger are (i) Internal tank temperature, (ii) Temperature inlet tube of the exchanger, and (iii) Pressure inside the tube. The proposed quadratic modeling function offers the possibility of predicting the optimal solution in the experiment space limited by the low and high levels of each input factor. The development sequence makes it possible to minimize the error by the method of least squares (R-Square). The model development tries to minimize the squared error deduced from the least-squares calculations of the estimated results concerning the numerical simulation results and/or the experimental observations. The minimization of the quadratic error requires the derivation of the quadratic error function which will lead to the identification of all factors αi, αii, αij of the equation.

The output response data is regressively adjusted by RSM to a first, second or n^{th} -order model, and the coefficients involved (β) are determined. Model validation is done by statistical analysis of the fitting accuracy using the least-squares technique, along with the Analysis of Variance (ANOVA)

to check the quality of the developed model. Following this sequence, the model expression is stated by the following equation:

$$T_o = 27.5111 - 1.788 \times P_1 + 2.583 \times T_h + 3.838 \times T_i + 0.544 \times {P_1}^2 - 0.941 \times P_1 \times T_h - 0.725 \times T_h \times T_i \quad (2)$$

This second-degree polynomial aligns with the results of the Pareto and the effect of independent variables and their significant interaction are shown in **Figs. 7, 8,** and **9**. The polynomial shows that the change in inlet temperature T_i has a major change in response due to the largest coefficient value of 3.838. Also, only one interaction is observed between T_h and T_i as previously justified in **Fig. 7**. It is also mentioned that the only second order factor is the pressure which supported by the curve plotted in **Fig. 8**, while the two factors T_h and T_i have a linear effect on the output response. Thus, the signs of the coefficients indicated in the model designate the sign of the effect. The coefficients of T_h and T_i have positive signs indicating that the evolution of T_o is proportional to T_h and T_i. Although the pressure has negative and positive signs, the evolution of T_o is affected inversely by increasing the inlet P_1. Increasing the inlet P_1 means more mass flow rate through the coil and in turn decrease in outlet temperature. Concerning the 3D surfaces of the sprains of T_o, three configurations have been implanted to define the evolution of T_o with the low level of the three independent variables. Also, three 2-D contour plots are generated for T_o at the low, center, and high levels of inlet temperature T_i.

Figures 11 a-f provide detail about 2D and 3D surfaces of T_o evolution for the study range of the independent variables. The shape of the curves are continuous linear along the axis T_h and T_i and parabolic along the axis P_1. These figures show the significant and major effect of T_i as well as the operating parameters specification to get a desired T_o value. **Figure 11** illustrates the different surfaces of the responses; these surfaces specify the magnitude of the three study factors to get a certain response T_o value. Since our model is linear, the optimal value of T_o is reached when the two temperatures T_i and T_h are maximized and the pressure P_1 is minimized. As shown in **Table 5**, the optimum value is found to be 36.6074 °C.

Table 5. Optimal values.

Goal : maximise T_o			
Factor	Low	High	Optimum
p_1	0.5	1.5	0.5
T_h	40	60	60
T_i	15	25	25
Optimum value of T_o :	36.6074°C		

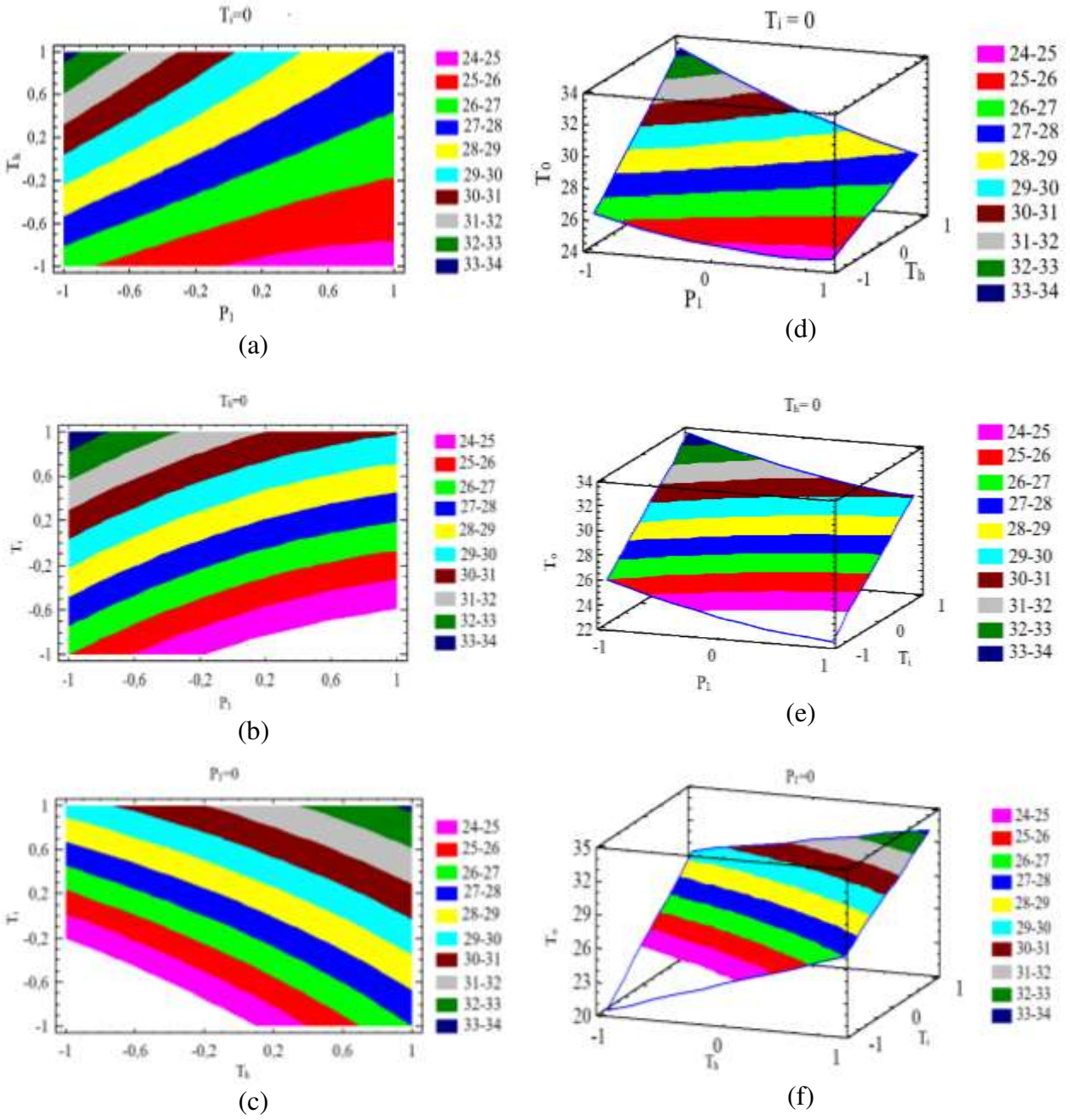

Fig. 11. The 2D and 3D contour surfaces of the temperature response against the variation of P_1, T_h, and T_i.

Conclusion

In this study, the effect of three non-dimensional input parameters on the exit temperature of a helical heat exchanger is evaluated. The considered independent parameters are the coil inlet temperature, the hot path temperature outside the coil, and the pressure inlet the tube. The study is carried out in two parts, the first part is the execution of 27 experimental runs representing the DOE full factorial of the three parameters at three levels of magnitude. While the second part is the application of the

statistical model RSM verified by ANOVA analysis. The main study results can be interpreted and concluded as follows:

- The predicted model describes more than 98% of the variability in the experimental data as indicated by the coefficient of determination.
- The ANOVA test shows that the performed experimental runs are well verified and the experimental results of the outlet temperature are undergoing a normal law. The analysis also indicates that the express model has an accuracy of more than 97%.
- In terms of effect and interaction, the major factor that has a significant impact on the outlet temperature is the temperature inlet to the exchanger tube, with an approximate rate of 30%. The effects of the inlet and hot bath temperatures are linear on the output response temperature while a quadratic effect for the actuating pressure has been observed. The mutual combination between the investigated parameters shows that there is no significant effect for the interaction term of inlet and hot bath temperatures while there is a strong correlation effect for the interaction of the inlet temperature and pressure.

Finally, the extracted equation for the output temperature of the heat exchanger is very important for the researchers and the manufacturers. It enables the calculation of the outlet temperature without reference to the physical and thermal properties of the used fluid. The equation has an accuracy that exceeds 97% and its configuration emphasizes the influencing degree of each factor on the temperature outlet.

Declarations

Ethical Approval

not applicable

Competing interests

-Tunis El Manar University

- National School of Engineers (ENIT) of Tunis

- Energy Research and Environment Unit

Authors' contributions

- Noureddine Toujani: Establishment of calculation program, illustrations of results and writing of manuscript

-Bahaa Saleh: Analysis, correction and initial review

- Nahla BOUAZIZ: final review

Funding

not applicable

Availability of data and materials

not applicable

References

[1] International Energy Agency (IEA), 2010. International Energy Outlook-Highlights.IEA, Washington D.C, USA.

[2] Wesley Herche. Solar energy strategies in the U.S. utility market. Renewable and Sustainable Energy Reviews 77 (2017) 590–595.

[3] C.G. Ozoegwu. The status of solar energy integration and policy in Nigeria. Renewable and Sustainable Energy Reviews 70 (2017) 457–471

[4] Aliyu, Abubakar Sadiq & Dada, Joseph O. & Adam, Ibrahim Khalil, 2015. Current status and future prospects of renewable energy in Nigeria. Renewable and Sustainable Energy Reviews, Elsevier, vol. 48(C), pages 336-346.

[5] Mohanty, Sthitapragyan & Patra, Prashanta K. & Sahoo, Sudhansu S. & Mohanty, Asit, 2017. Forecasting of solar energy with application for a growing economy like India: Survey and implication, Renewable and Sustainable Energy Reviews, Elsevier, vol. 78(C), pages 539-553.

[6] Omid Nematollahi, A feasibility study of solar energy in South Korea, Renewable and Sustainable Energy Reviews 77 (2017) 566–579

[7] Communication from the Commission to the European Parliament and the Council: Energy Efficiency 610 and its contribution to energy security and the 2030 Framework for climate and energy policy-Brussels, 611 23.7.2014 COM(2014) 520 final.

[8] Sarbu, Ioan & Sebarchievici, Calin. (2015). General review of solar-powered closed sorption refrigeration systems. Energy Conversion and Management. 105. 403-422. 10.1016/j.enconman.2015.07.084.

[9] Gingerich DB, Mauter MS. Quantity, Quality, and Availability of Waste Heat from United States Thermal Power Generation. Environ Sci Technol. 2015 Jul 21;49(14):8297-306. doi: 10.1021/es5060989. Epub 2015 Jun 30. PMID: 26061407.

[10] Cheng-Liang Chen, Po-Yi Li, and Si Nguyen Tien Le Industrial & Engineering Chemistry Research 2016 55 (12), 3262-3275 DOI: 10.1021/acs.iecr.5b03381

[11] Sunil Kumar Sansaniwal, Vashimant Sharma. Energy and exergy analyses of various typical solar energy applications: A comprehensive review. Renewable and Sustainable Energy Reviews. 82, Part 1, 2018, Pages 1576-1601. https://doi.org/10.1016/j.rser.2017.07.003.

[12] Bouaziz N, Lounissi D. Energy and exergy investigation of a novel double effect hybrid absorption refrigeration system for solar cooling. Int J Hydrog Energy 2015;40(39):13849–56.

[13]Gunhan T, Ekren O, Demir V, Sahin AS. Experimental exergetic performance evaluation of a novel solar assisted LiCl–H2O absorption cooling system. Energy Build 2014;68(Part A):138–46.

[14] F.R. Siddiqui, M.A.I. El-Shaarawi, S.A.M. Said, Exergo-economic analysis of a solar driven hybrid storage absorption refrigeration cycle, Energy Conversion and Management 80 (2014) 165-172. doi:10.1016/j.econman.2014.01.029.

[15] Gang P, Guiqiang L, Xi Z, Jie J, Yuehong S. Experimental study and exergetic analysis of a CPC-type solar water heater system using higher-temperature circulation in winter. Sol Energy 2012;86(5):1280–6.

[16] Shukla SK, Gupta SK. Performance evaluation of concentrating solar cooker under Indian climatic conditions. In: Proceedings of the Second international conference on energy sustainability, Jacksonville, Florida, USA; 10–14 Aug; 2008.

[17] Bolaji, Bukola. (2011). Exergetic Analysis of Solar Drying Systems. Natural Resources. 2. 92-97. 10.4236/nr.2011.22012.

[18]Fudholi A, Sopian KB, Othman MY, Ruslan MH. Energy and exergy analyses of solar drying system of red seaweed. Energy Build 2014;68(Part A):121–9.
[19] Naik PS, Palatel A. Energy and exergy analysis of a plane reflector integrated photovoltaic-thermal water heating system. ISRN Renew Energy 2014:1–9. http://dx.doi.org/10.1155/2014/180618.
[20] Wu, Jing Qiu, et al. Exergetic Analysis of a Solar Thermal Power Plant. Advanced Materials Research, vol. 724–725, Trans Tech Publications, Ltd., Aug. 2013, pp. 156–162. Crossref, doi:10.4028/www.scientific.net/amr.724-725.156.
[21] Ismael A.S. Ehtiwesh, Margarida C. Coelho, Antonio C.M. Sousa.Exergetic and environmental life cycle assessment analysis of concentrated solar power plants. Renewable and Sustainable Energy Reviews, Volume 56, April 2016, Pages 145-155
[22] Cau G, Cocco D. Comparison of medium size concentrating solar power plants based on parabolic through and linear Fresnel collectors. Energy Procedia2014; 45:101–110
[23] Yousefi, Hossein & Hamlehdar, Maryam & Tabasi, Sanaz & Noorollahi, Younes. (2017). Economic and Thermodynamic Evaluations of Using Geothermal Heat Pumps in Different Climate Zone.
[24] Dehghan B., Babak. (2017). Performance assessment of ground source heat pump system integrated with micro gas turbine: Waste heat recovery. Energy Conversion and Management. 152. 328-341. 10.1016/j.enconman.2017.09.058.
[25] Carotenuto A, Marotta P, Massarotti N, Mauro A, Normino G. Energy piles for ground source heat pump applications: comparison of heat transfer performance for different design and operating parameters. Applied Thermal Engineering 2017;124, 1492-1504.
[26] Zarrella, Angelo & De Carli, Michele & Galgaro, Antonio. (2013). Thermal performance of two types of energy foundation pile: Helical pipe and triple U-tube. Applied Thermal Engineering. 61(2). 301-310. 10.1016/j.applthermaleng.2013.08.011.
[27] Zhao, Qiang & Chen, Baoming & Liu, Fang. (2016). Study on the thermal performance of several types of energy pile ground heat exchangers: U-shaped, W-shaped and helical-shaped. Energy and Buildings. 133. 10.1016/j.enbuild.2016.09.055.
[28] Zhou H, Lv J, Li T. Applicability of the pipe structure and flow velocity of vertical ground heat exchanger for ground source heat pump. Energy Build 2016;117:109–119.
[29] Li, Y.; Mao, J.; Geng, S.; Xu, H.; Zhang, H. Evaluation of thermal short-circuiting and influence on thermalresponse test for borehole heat exchanger. Geothermics 2014,50, 136–147.
[30] Bauer D, Heidemann W, Müller-Steinhagen H, Diersch HJG. Thermal resistance and capacity models for borehole heat exchangers. Int J Energy Res. 2011;35(4):312–20.
[31] Al-Khoury, R. & Bonnier, P. & Brinkgreve, R.. (2005). Efficient finite element formulation for geothermal heating systems. Part I: Steady state. International Journal for Numerical Methods in Engineering. 63. 988 - 1013. 10.1002/nme.1313.
[32] Al-Khoury, R. & Bonnier, P.. (2006). Efficient finite element formulation for geothermal heating systems. Part II: Transient. International Journal for Numerical Methods in Engineering. 67. 725 - 745. 10.1002/nme.1662.
[33] He, Miaomiao & Rees, Simon & Shao, L.. (2011). Simulation of a domestic ground source heat pump system using a transient numerical borehole heat exchanger model. Journal of Building Performance Simulation. 4. 141-155. 10.1080/19401493.2010.513739.
[34] Comsol, ComsolMultiphysics, Introduction to Pipe Flow Module (Version 5.0); 2016.

[35] Florides, Georgios & Kalogirou, Soteris. (2007). Ground heat exchangers-A review of systems, models and applications. Renewable Energy. 32. 10.1016/j.renene.2006.12.014.
[36] Yang, Hongxing & Cui, Patrick & Fang, Zhaohong. (2010). Vertical-borehole ground-coupled heat pumps: A review of models and systems. Applied Energy. 87. 16-27. 10.1016/j.apenergy.2009.04.038.
[37] Esen, Mehmet & Ayhan, Teoman. (1996). Development of a model compatible with solar assisted cylindrical energy storage tank and variation of stored energy with time for different phase change materials. Energy Conversion and Management. 37. 1775-1785. 10.1016/0196-8904(96)00035-0.
[38] Shirvan, Kamel & Mamourian, Mojtaba & Mirzakhanlari, Soroush & Ellahi, Rahmat. (2016). Two phase simulation and sensitivity analysis of effective parameters on combined heat transfer and pressure drop in a solar heat exchanger filled with nanofluid by RSM. Journal of Molecular Liquids. 220. 888-901. 10.1016/j.molliq.2016.05.031.
[39] Shirvan, Kamel & Mamourian, Mojtaba & Mirzakhanlari, Soroush & Öztop, Hakan & Abu-Hamdeh, Nidal. (2016). Numerical simulation and sensitivity analysis of effective parameters on heat transfer and homogeneity of Al2O3 nanofluid in a channel using DPM and RSM. Advanced Powder Technology. 27. 10.1016/j.apt.2016.06.030.
[40] Shirvan, K. & Mamourian, Mojtaba & Mirzakhanlari, Soroush & Ellahi, Rahmat & Vafai, Kambiz. (2017). Numerical investigation and sensitivity analysis of effective parameters on combined heat transfer performance in a porous solar cavity receiver by response surface methodology. International Journal of Heat and Mass Transfer. 105. 811-825. 10.1016/j.ijheatmasstransfer.2016.10.008.
[41] Shirvan, Kamel & Mamourian, Mojtaba & Mirzakhanlari, Soroush & Ellahi, Rahmat. (2017). Numerical Investigation of Heat Exchanger Effectiveness in a Double Pipe Heat Exchanger Filled With Nanofluid: A Sensitivity Analysis by Response Surface Methodology. Powder Technology. 313. 99-111. 10.1016/j.powtec.2017.02.065.
[42] Kim, Hong-Min & Kim, Kwang-Yong. (2004). Design optimization of rib-roughened channel to enhance turbulent heat transfer. International Journal of Heat and Mass Transfer. 47. 5159-5168. 10.1016/j.ijheatmasstransfer.2004.05.035.
[43] Kim, Kwang-Yong & Lee, Young-Mo. (2007). Design Optimization of Internal Cooling Passage with V-shaped Ribs. Numerical Heat Transfer Part A-applications - NUMER HEAT TRANSFER PT A-APPL. 51. 1103-1118. 10.1080/10407780601112860..
[44] Zhang, Jiehai & Kundu, Jaydeep & Manglik, Raj. (2004). Effect of fin waviness and spacing on the lateral vortex structure and laminar heat transfer in wavy-plate-fin cores. International Journal of Heat and Mass Transfer. 47. 1719-1730. 10.1016/j.ijheatmasstransfer.2003.10.006.
[45] Polley, Graham. (2003). Optimal design of plate heat exchangers with and without pressure drop specification (By L. Wang and B. Sundén). Applied Thermal Engineering - APPL THERM ENG. 23. 2147-2148. 10.1016/S1359-4311(03)00169-8